ORIGINAL PAPER

Determination method of high-temperature characteristics of iron-ore sintering based on $n(Fe_2O_3)/n(CaO)$

Zheng-wei Yu[1] · Li-xin Qian[1] · Hong-ming Long[1,2] · Yi-fan Wang[1] · Qing-min Meng[1] · Tie-jun Chun[1]

Abstract

The high-temperature characteristics of iron ores play important roles in optimizing ore proportion of sintering, which are tested by using iron-ore fines and analytical reagent CaO as raw materials. Two calculation methods of CaO addition amount based on binary basicity (basicity method) and $n(Fe_2O_3)/n(CaO)$ (mole ratio method), respectively, were employed to evaluate the liquid phase fluidity (LPF) and the capability of calcium ferrite formation (CCFF) of iron ores. The results show that the rule of LPF of iron ores under the mole ratio method is different from that with basicity method. The LPF measured by basicity method has a linear positive correlation with the SiO_2 content, and there is no linear relationship between LPF and Al_2O_3 content or mass loss on ignition, which are inconsistent with the results of the previous study. And the results of CCFF with low SiO_2 content (< 3 wt.%) or high SiO_2 content (> 7 wt.%) based on basicity method cannot reflect the true CCFF. The mole ratio method could successfully solve this problem by reducing the effect of CaO addition amount changes caused by SiO_2 content of iron ores.

Keywords Iron-ore sintering · High-temperature characteristics · Liquid phase fluidity · Calcium ferrite · CaO addition amount

1 Introduction

With the development of large-scale blast furnace, the quality of sinter was required to improve continually for the smooth operation of blast furnace. Ultimately, the quality of sinter is decided by the properties of sintering raw materials, especially the high-temperature characteristics [1], such as assimilation property, liquid phase fluidity (LPF), strength of bonding phase and capability of calcium ferrite formation (CCFF). Generally, the sinter is consolidated by melt phase through adhering of the adjacent unreacted nucleus [2]. Therefore, the CCFF of iron ore

with CaO and the LPF after calcium ferrite is melted are extremely important for the quality of the sinter [3–5]. The liquid phase is the basis of sintering. If the LPF is too low during sintering, the ability of liquid-phase bonding around material reduces, and part of iron ore cannot be effectively bonded, which declines the yield of sinter [6, 7]. Calcium ferrite is one of the main bonding phases of sinter, and its content directly affects the strength and reduction in sinter. It has been reported that the LPF and CCFF have achieved good results in the optimization of sintering ore matching [8–11].

The LPF and CCFF are generally detected by using iron ore and analytical reagent CaO as raw materials. The binary basicity ($R_2 = w(CaO)/w(SiO_2)$) of iron ore–CaO mixture is fixed to decide the amount of CaO addition (hereinafter referred to as the basicity method). In this method, the addition amount of CaO is determined by the SiO_2 content of iron ore. When the LPF and CCFF of some special iron ores are measured by basicity method, the evaluation conclusions are often inconsistent with the actual sintering production. For example, Cara ore is a common imported ore in sintering plant, which is featured

✉ Li-xin Qian
ahutlxq@126.com

✉ Hong-ming Long
yaflhm@126.com

1 School of Metallurgical Engineering, Anhui University of Technology, Ma'anshan 243002, Anhui, China

2 Key Laboratory of Metallurgical Emission Reduction and Resources Recycling (Anhui University of Technology), Ministry of Education, Ma'anshan 243002, Anhui, China

with high iron grade and low SiO_2 content ($w(SiO_2) < 3$ wt.%). When the LPF and CCFF of Cara ore are detected by basicity method, it has a poor liquidity and not prominent CCFF [12]. However, Cara ore shows an excellent sintering performance in sintering practice; when a certain amount of Cara ore is added to sinter mix, the quality and yield indices of sinter are improved obviously. In addition, the iron ores with high SiO_2 content ($w(SiO_2) > 7$ wt.%) show excellent LPF and CCFF when the basicity method was used [12], but the practice of production shows that increasing the ratio of high-silica ore in sinter mix will reduce the grade of sinter and produce a lot of high-melting-point silicate. And the viscosity of liquid phase is increased, which results in bad fluidity and poor quality of sinter [3, 13]. Therefore, the evaluation results of iron ores based on basicity method are difficult to guide the optimization of ore matching effectively.

Although researchers have done a lot of experimental researches on the high-temperature characteristics of iron ore [6–13], most of these studies are carried out by means of fixed-sample binary basicity. Previous studies [14–16] show that during the actual production process, the sintering enterprises often need to use a variety of iron ores to maintain the SiO_2 mass fraction of the mixed ore in a certain range (4.5–5.5%) to maintain better sintering technology and economic indicators. Therefore, the addition of CaO in a fixed CaO ratio was proposed. However, during the formation of sintered liquid phase, the reaction of single ore in mixed ores with CaO is performed at a molar ratio. Not because of the high content of SiO_2 in some iron ores, more CaO will react with it. According to the above analysis of these issues, an improved CaO addition amount calculation method based on the mole ratio of Fe_2O_3 to CaO ($n(Fe_2O_3)/n(CaO)$) was proposed in this paper (hereinafter referred to as the mole ratio method) to reduce the adverse effect of SiO_2 content on the high-temperature characteristics. The LPF and CCFF of iron ores were studied by the basicity method and mole ratio method, respectively.

2 Experimental materials and methods

2.1 Raw materials

Common imported iron ores of China (including two limonite iron ores and five hematite iron ores) and analytically pure CaO reagent were used. Among them, Ore-A, Ore-E and Ore-F are hematite iron ores from Brazil, Ore-D and Ore-G are limonite iron ores from Australia, and Ore-B and Ore-C are hematite iron ores from Australia. Table 1 shows their main chemical compositions. The contents of SiO_2 in seven iron ores are different, in which, the Ore-A

Table 1 Main chemical compositions of iron ores (wt.%)

Raw material	TFe	SiO_2	CaO	Al_2O_3	MgO	FeO	LOI
Ore-A	64.57	2.12	0.04	1.52	0.04	0.99	2.57
Ore-B	61.22	3.72	0.40	2.54	0.20	0.65	4.95
Ore-C	62.36	4.83	0.10	2.25	0.40	0.54	2.50
Ore-D	57.90	5.61	0.23	2.75	0.07	0.64	7.78
Ore-E	62.13	6.11	0.08	1.90	0.07	1.08	2.70
Ore-F	62.35	7.21	0.10	1.15	0.08	0.89	2.21
Ore-G	52.24	11.86	0.20	4.08	0.06	0.63	7.88

LOI Mass loss of ignition at 900 °C for 3 h

has the lowest content of SiO_2, while the Ore-G has the highest one.

2.2 Experimental method

2.2.1 LPF of iron ores

In this work, the liquid phase fluidity index was used to evaluate the LPF of iron ores. The LPF index was achieved by comparing the area of the liquid phase before and after sinter tests. The detailed procedure was presented as follows: (1) Firstly, all iron ores were ground to − 0.074 mm by using a sealed crusher and they were dried. (2) According to the content of $w(SiO_2)$ of single iron ore, R_2 was set at 4.0 to add analytically pure CaO reagent [17]. Or according to the content of $w(Fe_2O_3)$ in single iron ore, the mole ratio of $n(Fe_2O_3)/n(CaO)$ was set at 1.5 to add analytically pure CaO reagent. Then, the samples were mixed. (3) About (0.80 ± 0.01) g of fine mixture was shaped into tablets with a diameter of 8 mm by using steel molds under a pressure of 15 MPa. (4) The tablet was put on an alloy plate, and then it was sintered in the micro-sinter equipment, as shown in Fig. 1. In order to enable a close simulation of the real sintering process that arose in a sintering machine [18], the standard temperature profile used is shown in Table 2. (5) After the experiment, the cake sample was taken out and LPF index was calculated as shown in Eq. (1) [12].

$$F = \frac{S_1 - S_0}{S_0} \tag{1}$$

where F is the liquid phase fluidity index; S_1 is the flowing area after sinter experiment, mm²; and S_0 is the original area before sinter experiment, mm².

2.2.2 CCFF of iron ores

The area percentage of calcium ferrite formation was used to evaluate the CCFF of iron ores. The experimental
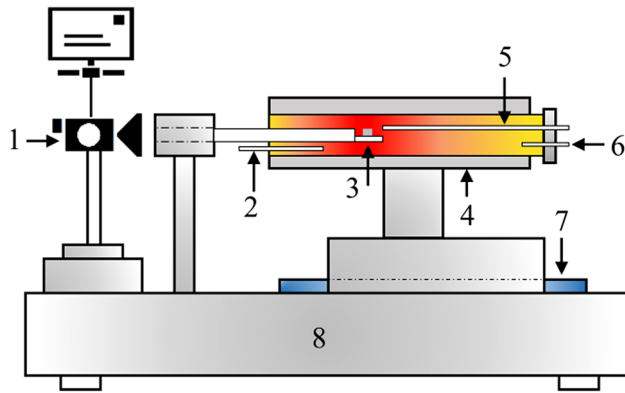
Fig. 1 Device of micro-sintering experiment. 1 Camera system; 2 furnace temperature thermocouple; 3 stage and sample; 4 furnace body; 5 sample temperature thermocouple; 6 gas supply system; 7 track; 8 base

Table 3 Results of liquid phase fluidity index of iron ores

Raw material	$n(Fe_2O_3)/n(CaO) = 1.5$	$R_2 = 1.5$
Ore-A	3.45	0
Ore-B	2.13	0.35
Ore-C	2.56	2.22
Ore-D	1.23	2.99
Ore-E	2.15	3.78
Ore-F	2.28	5.01
Ore-G	0	5.68

Table 4 CaO content, R_2 and $n(Fe_2O_3)/n(CaO)$ with basicity method and mole ratio method

Raw material	Basicity method			Mole ratio method		
	CaO/ %	$n(Fe_2O_3)/ n(CaO)$	R_2	CaO/ %	$n(Fe_2O_3)/ n(CaO)$	R_2
Ore-A	7.88	3.76	4.0	17.89	1.50	10.0
Ore-B	12.98	2.04	4.0	16.79	1.50	5.3
Ore-C	16.19	1.60	4.0	17.31	1.50	4.3
Ore-D	18.50	1.28	4.0	16.12	1.50	3.4
Ore-E	19.73	1.25	4.0	17.14	1.50	3.3
Ore-F	22.45	1.07	4.0	17.16	1.50	2.8
Ore-G	32.65	0.55	4.0	14.83	1.50	1.4

procedures of the CCFF were almost the same to the LPF experimental steps (1)–(4). However, in step (2), R_2 was set at 2.0 [17] or the mole ratio of $n(Fe_2O_3)/n(CaO)$ was set at 3. Generally speaking, the sinter grade was 56–58% in sintering process, and R_2 of the sinter was always about 1.8–2.0; on the case that the SiO_2 content of the sinter materials was 4.5–5.0 wt.%, the calculated value of $n(Fe_2O_3)/n(CaO)$ of sinter mix was 2.8–3.6. Thus, the mole ratio of $n(Fe_2O_3)/n(CaO)$ was set at 3. After the step (4), the sintering tablets were prepared for mineralogical sample; then, its mineralogical structure was observed using a metallographic microscope (Axio Scope A1) and the CCFF was calculated by a multi-phase content measurement module that comes with the metallographic microscope. The sample of mineral phase has a diameter of 8 mm and total area of about 0.5024 cm^2.

3 Results and discussion

3.1 Effect of calculation method of CaO addition amount on LPF index

In essence, the main difference between the basicity method and mole ratio method for sintering LPF index is the calculation method of CaO addition amount. Table 3 shows the effect of calculation methods of CaO addition

amount on LPF index of iron ores. It is indicated that the LPF index of iron ores has a distinct difference using two calculation methods of CaO addition amount.

In the present study, the Ore-A has the lowest content of SiO_2, while the Ore-G has the highest one. When the basicity method was used for Ore-A, the LPF index is 0, the lowest of the seven iron ores. While the mole ratio method was used, the LPF index of Ore-A is up to 3.45, the highest among seven iron ores. However, the experimental results of Ore-G were opposite to that of Ore-A. The LPF index was 5.68 under the basicity method and 0 under the mole ratio method, respectively.

Table 4 shows the calculated results of CaO content, R_2 and $n(Fe_2O_3)/n(CaO)$ of the mixture samples with basicity method and mole ratio method. When the basicity method

Table 2 Temperature system and atmosphere of micro-sintering experiment [12, 18]

Temperature/°C	RT to 600	600–1000	1000–1150	1150–1280	1280	1280–1150	1150 to RT
Atmosphere	Air	Nitrogen	Nitrogen	Nitrogen	Nitrogen	Air	Air
Time/min	4	3	1.5	1.5	4	2	22

RT Room temperature; and gas flow rate is 3 L/min

was used, the $n(Fe_2O_3)/n(CaO)$ in corresponding sample was reduced from 3.76 to 0.55 after adding CaO with the increase in SiO_2 content of iron ores from 2.21 to 11.86 wt.%. According to the liquid phase formation mechanism and thermodynamics of sintering process [18], calcium ferrite (CF), silico-ferrite of calcium (SFC) and complex silico-ferrite of calcium and aluminum (SFCA) were the main low-melting-point minerals and melt phase in high basicity sinter. In Table 4, when the sample of Ore-A with $n(Fe_2O_3)/n(CaO)$ of 3.76 was sintered, only a small amount of low-melting-point CF, SFC or other eutectic mixtures were generated and a great deal of remaining solid Fe_2O_3 had a framework support in the sample, which resulted in a poor LPF index. For other iron ores, with the increase in SiO_2 content, the addition amount of CaO is increased gradually. CaO is the basis of sintered liquid phase, and more CaO addition prompts the production of low-melting-point eutectic mixtures. Then, the number of remaining solids was decreased in the liquid phase and the liquid viscosity became lower, so that the LPF index was gradually enlarged.

The main liquid phase in sintering process is iron–calcium complex, and the reaction between Fe_2O_3 and CaO is performed at a certain mole ratio. Thus, the addition of CaO based on mole ratio method ensures that each iron ore has the same probability of producing iron–calcium complex, and the effect of other physical and chemical properties of iron ore on LPF index can be investigated.

Figure 2 shows the analysis results of correlativity of SiO_2 content with LPF index for basicity method and mole ratio method. For basicity method, LPF index increased with the increase in SiO_2 content and the adjusted R^2 is 0.794. For mole ratio method, LPF index decreased with the increase in SiO_2 content and the adjusted R^2 is 0.713. Wu et al. [19] found that when the $n(Fe_2O_3)/n(CaO)$ value was set at 1.5 and the SiO_2 content was above 2.5 wt.%, the
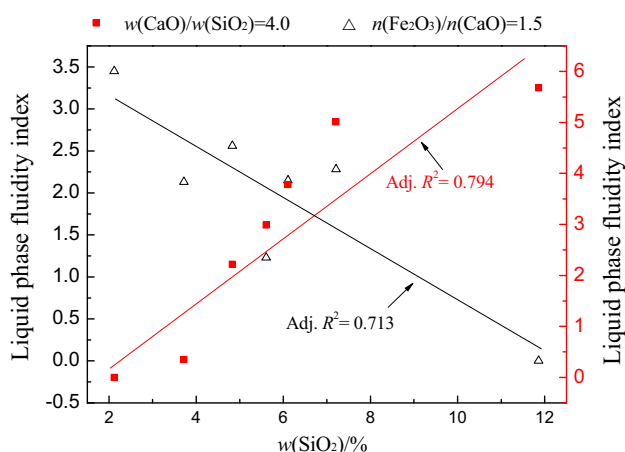
LPF index decreased with increasing the SiO_2 content. The main reason is that SiO_2 is the formation material of the silicate network, which can increase the liquid viscosity. And SiO_2 can reduce the production of sintered liquid phase when its content exceeds 5 wt.% [20]. In this study, the SiO_2 content of six iron ores, except the Ore-A, is greater than 2.5 wt.%. Thus, the results of LPF index based on mole ratio method are more similar to those of previous studies [19, 20].

Figure 3 shows the analysis results of correlativity of Al_2O_3 content with LPF index for basicity method and mole ratio method. Al_2O_3 content of seven iron ores is between 1.15 and 4.08 wt.%. LPF index decreased with the increase in Al_2O_3 content, and the adjusted R^2 is 0.727 for mole ratio method. There is no linear relationship between LPF index measured by basicity method and the Al_2O_3 content, because the adjusted (adj.) R^2 is $-$0.083. Figure 4 shows the analysis results of correlativity of LOI with LPF index for basicity method and mole ratio method, which is similar to the analysis result of Al_2O_3. When the LOI of seven iron ores increases from 2.21 to 7.88 wt.%, the LPF index measured by mole ratio method has a linear negative relationship with LOI and the adjusted R^2 is 0.655, whereas there is also no linear relationship for basicity method, and the adjusted R^2 is $-$0.116.

Previous studies [3, 21–26] have indicated that the LPF index of iron ore shows a decreasing trend with the increase in Al_2O_3 and LOI. For Al_2O_3, it will block the diffusion of Fe_2O_3 and CaO in sintered liquid phase, thereby decreasing the formation speed of eutectic mixtures. Al_2O_3 also promoted the formation of silicate network structures, which could increase the viscosity of melt and reduce the production of sintered liquid phase [21–25]. In addition, the affinity between CaO and Al_2O_3 is higher than that between CaO and Fe_2O_3 because of the lower Gibbs free energy change of $CaO \cdot 2Al_2O_3$, which decreases

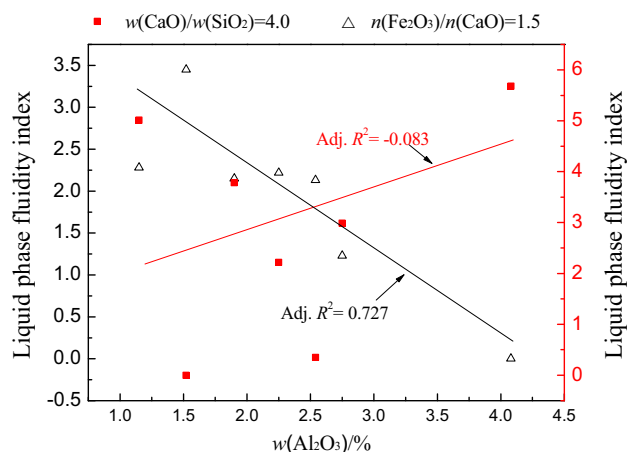Fig. 2 Correlativity of SiO_2 with LPF index of iron ores

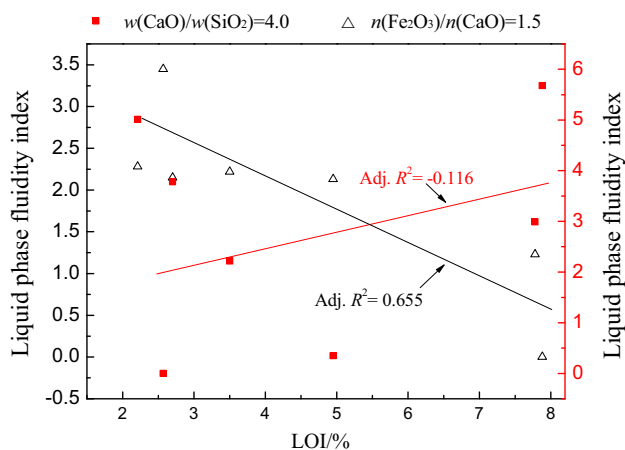Fig. 3 Correlativity of Al_2O_3 with LPF index of iron ores

Fig. 4 Correlativity of LOI with LPF index of iron ores

the formation rate of calcium ferrite [12]. For LOI, thermal decomposition of crystal water and carbonate happens, leaving a lot of pores in the iron ore during the sintering. Then, the pores were filled with eutectic mixtures liquid, resulting in a corresponding decrease in the flow area [26]. Therefore, the results of mole ratio method are more similar to those of previous studies than those of basicity method, and are closer to actual sintering.

3.2 Effect of calculation method of CaO addition on CCFF

Figure 5 shows the results of CCFF of seven iron ores with basicity method and mole ratio method. The largest difference of CCFF appears in Ore-A and Ore-G. When the basicity method and mole ratio method were adopted, the CCFF was 31.2% and 74.3% for Ore-A, while it was 88.7% and 5.0% for Ore-G, respectively. The CCFF is affected by Fe_2O_3, SiO_2 Al_2O_3 and LOI at the same time. When the natural iron ores are used as raw materials, the relationship between single factor and CCFF is not obvious. Therefore,
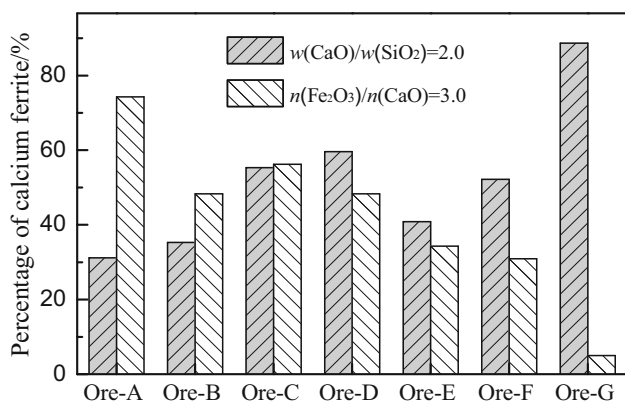

Fig. 5 Effect of calculation method of CaO addition on CCFF of iron ores

the CCFF of Ore-A and Ore-G was mainly analyzed in this paper. In addition, it is suggested that multiple influence factors should be multiplied by its influence factor weight to take cumulative summation and get a comprehensive impact index. And the relationship between the comprehensive impact index and CCFF needs to be studied further.

Figure 6 shows the results of energy-dispersive spectrometry analysis of Ore-A and Ore-G with two different methods. The mineralogical structure of Ore-A briquette roasted with the mole ratio method is shown in Fig. 6a. The main mineral is calcium ferrite, and it appeared plank or bulk in the microstructure of sample. The calcium ferrite amount is great, and the calcium ferrite grains are connected with each other. In addition, there is only a small quantity of hematite grains embedded in the calcium ferrite bulk. Figure 6b shows the mineralogical structure of Ore-A briquette roasted using the basicity method. It can be observed that the calcium ferrite grains are unequally distributed at the edge of hematite grains, and the crystalline grains are imperfectly developed. Some hematite grains are melted by calcium ferrite. Comparatively, there are more pores in the roasted sample.

The mineralogical photograph of Ore-G briquette roasted using mole ratio method is presented in Fig. 6c. It can be seen that there is precious little calcium ferrite distributed among the hematite grains, and lots of silicate grains are unequally distributed in hematite grains. Figure 6d shows the Ore-G briquette roasted using basicity method; it is observed that calcium ferrite grains are generated in abundance and well crystallized. Same as those in Fig. 6a, only a small number of hematite grains remained in calcium ferrite grains.

Table 5 shows the main chemical components of the mixture samples after addition of CaO based on basicity method and mole ratio method. When the basicity method was adopted for different iron ores, the maximum deviation of CaO content was 15.23 wt.%, while the CaO content was relatively stable and the maximum deviation is only 1.89 wt.% with the mole ratio method for the same mixture samples. The basicity method is more unstable for the effect on CaO content of the sample.

The experimental result shows that the CCFF of Ore-A is very ordinary by using basicity method. The reason is that the $n(Fe_2O_3)/n(CaO)$ value of the mixture samples is 7.6, and there is not enough amount of CaO reacting with Fe_2O_3, which makes a great deal of Fe_2O_3 remained. When the $n(Fe_2O_3)/n(CaO)$ value is set to 3.0, the addition amount of CaO is adequate in the roasted sample, and the calcium ferrite is generated in large quantities.

Ding et al. [27, 28] found that when the $n(Fe_2O_3)/n(CaO)$ value was 1.0 in the roasted sample, the new minerals formed changed along SFC,
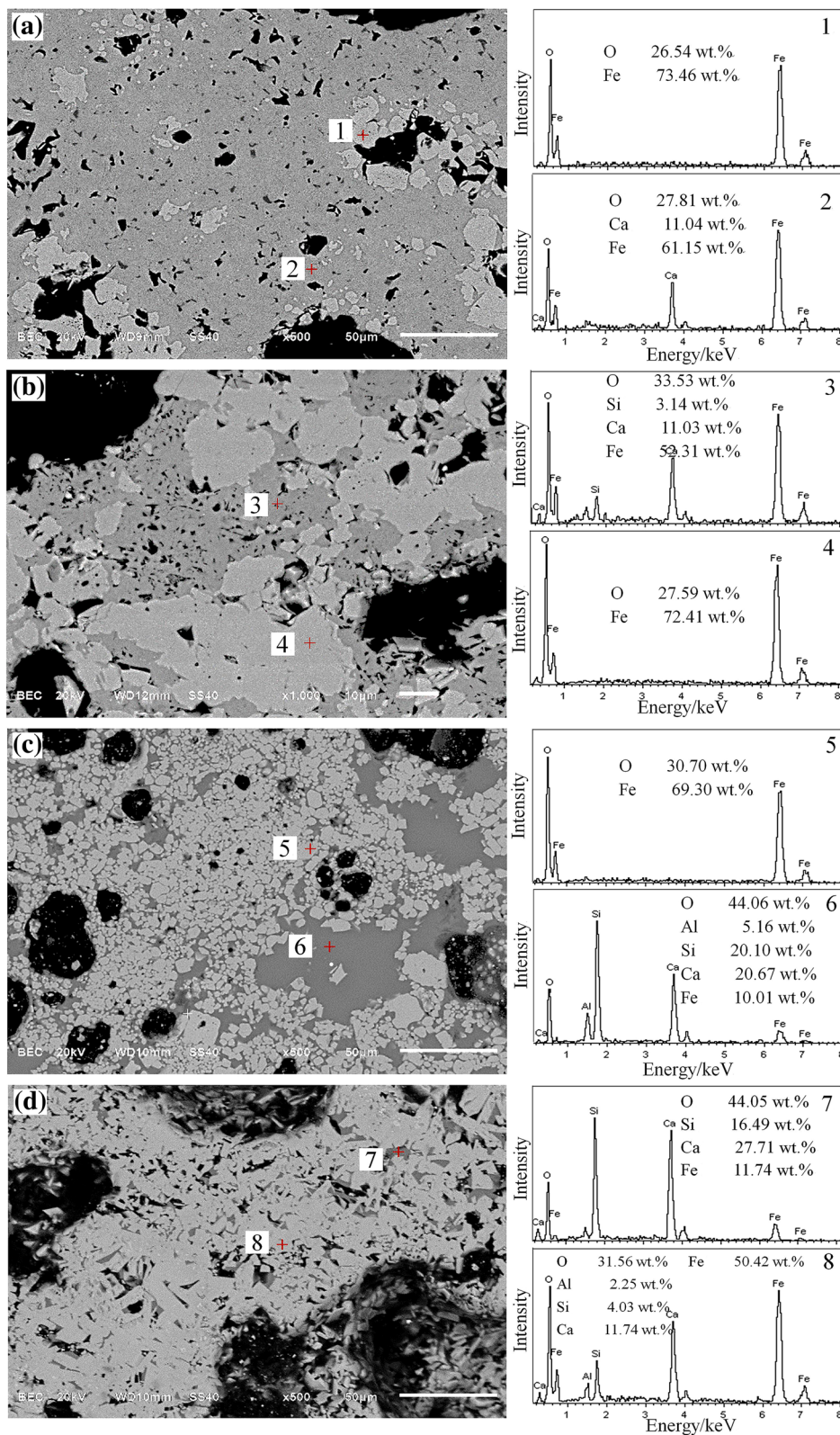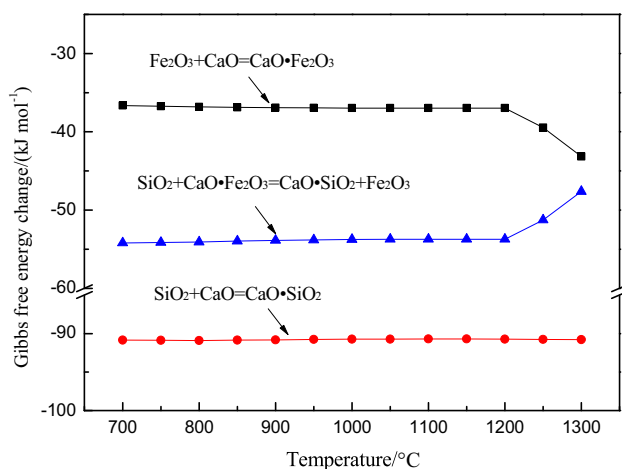
Fig. 6 Backscattered electron micrograph of quenched sample and energy-dispersive spectrometry results of key phases. **a** Ore-A, mole ratio method; **b** Ore-A, basicity method; **c** Ore-G, mole ratio method; **d** Ore-G, basicity method. 1, 4 and 5 are hematite; 2 is CF; 3 is SFC; 6 and 7 are silicate; 8 is SFCA

Table 5 Main chemical compositions of mixture sample based on basicity method and mole ratio method (wt.%)

Raw material	Basicity method			Mole ratio method		
	Fe_2O_3	CaO	SiO_2	Fe_2O_3	CaO	SiO_2
Ore-A	89.71	4.13	2.09	84.40	9.81	1.96
Ore-B	82.30	6.68	3.53	80.26	8.99	3.44
Ore-C	82.14	8.87	4.48	81.64	9.43	4.46
Ore-D	74.98	10.05	5.13	76.13	8.67	5.21
Ore-E	79.25	10.99	5.53	80.71	9.34	5.63
Ore-F	77.90	12.66	6.38	80.86	9.34	6.62
Ore-G	60.86	19.36	9.76	69.50	7.92	11.15

$SFC + Fe_2O_3 + CaO \cdot SiO_2$ to $Fe_2O_3 + CaO \cdot SiO_2$ with increasing addition of SiO_2 from 0.05 to 21.74 wt.%. With the maximum SFC produced in sample, the amount of SiO_2 addition was 10.64 wt.%. In the present experiment, when the basicity method was used for Ore-G, the $n(Fe_2O_3)/n(CaO)$ was 1.1 and $w(SiO_2)$ was 9.76 wt.% in the corresponding roasted sample. Therefore, most of SiO_2 reacted with CaO, Al_2O_3 and Fe_2O_3 to form SFC or SFCA and only a few $CaO \cdot SiO_2$ precipitated after crystallization, as shown in Fig. 6d. When the mole ratio method was adopted, the $n(Fe_2O_3)/n(CaO)$ was 3.0 in the corresponding roasted samples. In this case, the ability of reaction between CaO and SiO_2 is greater than that between CaO and Fe_2O_3 because compared with the CF formation reaction, the formation reaction of $CaO \cdot SiO_2$ shows a greater negative value of Gibbs free energy change, as shown in Fig. 7 [28].

Hence, CaO is more likely to crystallize with SiO_2 and form $CaO \cdot SiO_2$, which makes the amount of calcium ferrite

grains being meager [29]. That can explain why there are a lot of silicate phases in Fig. 6c. Generally, the reaction probability that each of the iron ores forms calcium ferrite with the additive CaO is the same in the actual process of sintering. The high SiO_2 content will not cause more CaO to react with it. Therefore, it can be concluded that Ore-A belongs to the iron ore which has strong calcium ferrite formation ability, while the CCFF of Ore-G is not prominent. The experimental results of the molar ratio method are more reasonable.

4 Conclusions

1. The rule of LPF index of iron ores under the mole ratio method is different from that with basicity method. When the mole ratio method is used, the LPF index of iron ore decreases with the increase in gangue content. The molar ratio method is more in line with the liquid phase formation behavior of iron ore during the actual sintering process.

2. Compared with basicity method, the CaO addition amount on the basis of mole ratio method is closer to the real sintering system, which can more reasonably reflect the ability of iron oxides to react with CaO in the sintering process.

3. The high-temperature characteristics data of iron ore obtained by mole ratio method can be used as a guide for optimization of ore blending in iron-ore sintering, and it is expected to provide some technical guidance for improving the quality index of sintering products.

Fig. 7 Relationships between Gibbs free energy change and temperature of the reactions. Thermochemical data were taken from the software of HSC Chemistry 6.0

References

[1] B.X. Su, J.L. Zhang, J. Chang, G.W. Wang, C.L. Wang, X.M. Che, Iron and Steel 46 (2011) No. 9, 22–28.

[2] W. Wang, M. Deng, R.S. Xu, W.B. Xu, Z.L. Ouyang, X.B. Huang, Z.L. Xue, J. Iron Steel Res. Int. 24 (2017) 998–1006.

[3] J.Q. Yin, X.W. Lv, S.L. Xiang, C.G. Bai, B. Yu, ISIJ Int. 53 (2013) 1571–1579.

[4] L. Yao, S. Ren, X.Q. Wang, Q.C. Liu, J.L. Zhang, B.X. Su, Metall. Res. Technol. 114 (2017) 204.

[5] J. Zhang, X.M. Guo, Y.H. Qi, D.L. Yan, J. Iron Steel Res. Int. 22 (2015) 288–296.

[6] G.P. Luo, S.L. Wu, X.B. Jia, X.G. Duan, Z.Z. Hao, J. Iron Steel Res. 25 (2013) No. 10, 10–13.

[7] J. Peng, L. Zhang, L.X. Liu, S.L. An, Metall. Mater. Trans. B 48 (2017) 538–544.

[8] D. Oliveira, S.L. Wu, Y.M. Dai, J. Xu, H. Chen, J. Iron Steel Res. Int. 19 (2012) No. 6, 1–5.

[9] J. Zhang, X.M. Guo, X. J. Huang, J. Iron Steel Res. Int. 19 (2012) No. 10, 1–6.

[10] S.L. Wu, Y. Liu, J.X. Du, K. Mi, H. Lin, J. Univ. Sci. Technol. Beijing 24 (2002) 254–257.

[11] X.Y. Li, B.X. Su, L.G. Xia, J.L. Zhang, H.W. Guo, J. Iron Steel Res. Int. 22 (2015) 478–486.

[12] S.L. Wu, G.L. Zhang, S.G. Chen, B. Su, ISIJ Int. 54 (2014) 582–588.

[13] X.W. Lv, C.G. Bai, Q.Y. Deng, X.B. Huang, G.B. Qiu, ISIJ Int. 51 (2011) 722–727.

[14] S.L. Wu, B. Su, Y.H. Qi, Y. Li, B.B. Du, Chin. J. Eng. 40 (2018) 321–329.

[15] L.H. Hsieh, ISIJ Int. 45 (2005) 551–559.

[16] Z.L. Chen, J.L. Zhang, Y.P. Zhang, Z.W. Yan, D. Wang, B. Gao, Iron and Steel 51 (2016) No. 12, 8–14.

[17] S.L. Wu, Y.D. Pei, H. Chen, P. Peng, F. Yang, J. Univ. Sci. Technol. Beijing 30 (2008) 1095–1100.

[18] M. Zhou, T. Jiang, S.T. Yang, X.X. Xue, Int. J. Miner. Process. 142 (2015) 125–133.

[19] S.L. Wu, J.C. Bei, J. Zhu, B. Su, W. Huang, J. Iron Steel Res. 27 (2015) No. 9, 7–13.

[20] Q. Wei, X.M. Mao, H.B. Shen, Baosteel Tech. Res. 11 (2017) No. 3, 7–11.

[21] T.J. Chun, H.M. Long, J.X. Li, Sep. Sci. Technol. 50 (2015) 760–766.

[22] S.W. Kim, J.W. Jeon, I.K. Suh, S.M. Jung, Ironmak. Steelmak. 43 (2016) 500–507.

[23] G.L. Zhang, S.L. Wu, S.G. Chen, B. Su, Z.G. Que, C.G. Hou, Int. J. Miner. Metall. Mater. 21 (2014) 962–968.

[24] T.L. Li, C.Y. Sun, X.Y. Liu, S. Song, Q. Wang, Ironmak. Steelmak. 45 (2018) 755–763.

[25] H.M. Long, X.J. Wu, T.J. Chun, Z.X. Di, B. Yu, Metall. Mater. Trans. B 47 (2016) 2830–2836.

[26] W.Q. Huang, X.X. Zhang, Y.X. Liu, Z.W. Zhang, J. Iron Steel Res. 28 (2016) No. 7, 13–19.

[27] X. Ding, X.M. Guo, Metall. Mater. Trans. B 46 (2015) 1742–1750.

[28] X. Ding, X.M. Guo, C.Y. Ma, K. Tang, Y.D. Zhao, Metall. Mater. Trans. B 46 (2015) 1146–1153.

[29] G.P. Luo, S.L. Wu, G.J. Zhang, Y.C. Wang, J. Iron Steel Res. Int. 20 (2013) No. 3, 18–23.